

On the possible roles of N-terminal His-rich domains of Cu,Zn SODs of some Gram-negative bacteria

Dávid Árus^a, Attila Jancsó^a, Dániel Szunyogh^a, Ferenc Matyuska^a, Nóra Veronika Nagy^c,
Eufrozina Hoffmann^b, Tamás Körtvélyesi^b, Tamás Gajda^{a,*}

^a*Department of Inorganic and Analytical Chemistry, University of Szeged, Szeged, Hungary,*

^b*Department of Physical Chemistry and Materials Science, University of Szeged, Szeged,
Hungary*

^c*Institute of Structural Chemistry, Chemical Research Center, Budapest, Hungary*

**Corresponding author.*

E-mail: gajda@chem.u-szeged.hu (T. Gajda), Tel.: (+36)-62-544054, Fax: (+36)-62-420505

Abstract

The Cu,Zn superoxide dismutases (Cu,Zn SOD) isolated from some Gram-negative bacteria possess a His-rich N-terminal metal binding extension. The N-terminal domain of *Haemophilus ducreyi* Cu,Zn SOD has been previously proposed to play a copper(II)-, and may be a zinc(II)- chaperoning role under metal ion starvation, and to behave as a temporary (low activity) superoxide dismutating center if copper(II) is available. The N-terminal extension of Cu,Zn SOD from *Actinobacillus pleuropneumoniae* starts with an analogous sequence (HxDHxH), but contains considerably fewer metal binding sites. In order to study the possibility of the generalization of the above mentioned functions over all Gram-negative bacteria possessing His-rich N-terminal extension, here we report thermodynamic and solution structural analysis of the copper(II) and zinc(II) complexes of a peptide corresponding to the first eight amino acids (HADHDHKK-NH₂, **L**) of the enzyme isolated from *A. pleuropneumoniae*. In equimolar solutions of Cu(II)/Zn(II) and the peptide the MH₂**L** complexes are dominant in the neutral pH-range. **L** has extraordinary copper(II) sequestering capacity ($K_{D,Cu} = 7.4 \times 10^{-13}$ M at pH 7.4), which is provided only by non-amide (side chain) donors. The central ion in CuH₂**L** is coordinated by four nitrogens {NH₂,3N_{im}} in the equatorial plane. In ZnH₂**L** the peptide binds to zinc(II) through a {NH₂,2N_{im},COO⁻} donor set, and its zinc binding affinity is relatively modest ($K_{D,Zn} = 4.8 \times 10^{-7}$ M at pH 7.4). Consequently, the presented data do support a general chaperoning role of the N-terminal His-rich region of Gram-negative bacteria in copper(II) uptake, but do not confirm similar function for zinc(II). Interestingly, the complex CuH₂**L** has very high SOD-like activity, which may further support the multifunctional role of the copper(II)-bound N-terminal His-rich domain of Cu,Zn SODs of Gram-negative bacteria. The proposed structure for the MH₂**L** complexes have been verified by semiempirical quantum chemical calculations (PM6), too.

Keywords: Cu,Zn SOD, copper(II), zinc(II), peptid complexes, histidine

Introduction

Cu,Zn superoxide dismutases (Cu,Zn SODs) are important components of the antioxidant defence of aerobic organisms since they catalyze the disproportionation of superoxide anion into oxygen and hydrogen peroxide [1]. These enzymes can be found in all eukaryotic cells and in the periplasm of several bacteria, where they play a role in protection against superoxide generated outside the cytoplasm, for example by phagocytic cells [2]. The increasing number of structurally characterized prokaryotic Cu,Zn superoxide dismutases show a considerable structural variability between proteins from different bacteria, therefore individual enzyme variants may exhibit unique properties [3-8]. Such species-specific differences include alteration in the quaternary structure [3,4], mutations in the active site ligands [5-7], deletion or insertion in the major enzyme loops [6,7], or the introduction of additional domains at the N- or C-terminus of the enzyme [8]. The Cu,Zn SODs from a few Gram-negative bacteria possess histidine-rich N-terminal extensions, which show typical features of high affinity divalent metal binding domains [8].

The ability of bacteria to grow in different environments and, in particular, within the infected host is critically dependent on their ability to obtain sufficient amounts of transition metals [9] to activate their protective enzymes against the oxidative burst of the host phagocytes. Therefore, the identification of N-terminal metal binding domains exclusively in Cu,Zn SODs isolated from bacterial pathogens (*e.g. Haemophilus spp, Actinobacillus pleuropneumoniae, Neisseria meningitidis, Yersina pestis*) strongly suggest that their function is to promote metal recruitment in an environment which is poor of free metal ions. The Cu,Zn SODs of certain bacteria (*e.g. H. parainfluenzae, H. influenzae, N. meningitidis*) possess an N-terminal HxH sequence [8], a well-known high affinity copper(II) binding site (ATCUN motif) found in the N-terminus of several naturally occurring copper-binding proteins, such as human serum albumin [10]. Further interesting examples of such metal

binding regions are present in the enzymes isolated from *Haemophilus ducreyi* and *Actinobacillus pleuropneumoniae*. The former is the pathogen responsible of a genital ulcerative disease (chancroid), the latter causes the contagious porcine pneumonia, a veterinary pathogen of major economic significance. The N-terminal domain of *H. ducreyi* Cu,Zn SOD is constituted by the juxtaposition of a histidine- and a methionine-rich sequence (HGDHMHNHDTKMDTMSKDMMSME....) [7,8]. Both subdomains are able to bind copper, but the histidine-rich region has a marked preference for Cu(II) binding, while the methionine-rich region preferentially binds Cu(I) [11]. Copper bound to the above peptide can be transferred to the active site of the N-terminal deleted apo-SOD, suggesting that this sequence facilitates the metal transfer to the active site [11]. Recently, we studied the metal binding ability of the N-terminal histidine-rich fragment (H₂N-HGDHMHNHDTK-OH) of this enzyme [12]. As a consequence of its highly versatile multidentate nature, this peptide binds zinc(II) and copper(II) with very high affinity ($K_{D,Zn} = 1.6 \times 10^{-9}$ M and $K_{D,Cu} = 5.0 \times 10^{-12}$ M at pH 7.4) and appears to be the strongest non-amide utilizing copper(II) and zinc(II) chelator among the His-rich peptides so far investigated, which supports the proposed copper(II) chaperoning role of the N-terminal His-rich region of *H. ducreyi* Cu,Zn SOD, and indicates similar function in the zinc(II) uptake, too [12].

Although, the first six amino acids has analogous sequence (HxDHxH), the Cu,Zn SOD from *Actinobacillus pleuropneumoniae* has different N-terminal extension (HADHDHKKADNSSVE..., [8]), the methionine-rich sequence is completely absent and contains only three histidine units (instead of four in *H. ducreyi* Cu,Zn SOD). If the above mentioned chaperoning role of the N-terminal His-rich region of Gram-negative bacteria can be generalized, the N-terminal fragment of Cu,Zn SOD from *A. pleuropneumoniae* should have comparable metal binding ability with the corresponding *H. ducreyi* peptide, in spite of the reduced number of the available donor sites.

In order to study the possibility of this generalization, here we report thermodynamic and solution structural analysis of the copper(II) and zinc(II) complexes of a peptide corresponding to the first eight amino acids (HADHDHKK-NH₂, **L**) of the enzyme isolated from *A. pleuropneumoniae*. Since the copper(II) complex of the *H. ducreyi* peptide formed in the neutral pH range has significant SOD-like activity [12], which may suggest multifunctional role of the copper(II)-bound N-terminal His-rich domain, this behavior has been studied for the presently studied complexes, too.

2. Materials and methods

Copper(II) and zinc(II) chloride (Fluka) solutions were standardized complexometrically. pH-metric titrations were performed by NaOH (Fluka) standard solution. Fmoc-amino acids, 2-(1H-benzotriazole-1-yl)-1,1,3,3-tetramethyluronium hexafluorophosphate (HBTU) and N-hydroxybenzotriazole (HOBt) were Novabiochem products. N,N-diisopropylethylamine, diethylether (Sigma), triisopropylsilane, piperidine (Aldrich), pyridine (Merck), acetic anhydride (Fluka), trifluoroacetic acid (Riedel-de Haën), 1-methyl-2-pyrrolidone (NMP), N,N-dimethyl-formamide, dichloromethane, methanol (Molar Chemicals), and acetonitrile (Scharlau) were used without further purification.

2.1 Synthesis of HADHDHKK-NH₂ peptide (**L**)

The peptide was prepared by solid phase peptide synthesis using the Fmoc methodology (Fmoc = 9-fluorenylmethoxycarbonyl). Rink Amide AM (Novabiochem) was used as a solid support. The amino acid building blocks were applied in 4-fold excess over the capacity of the resin. The amino acid residues were coupled to each other (and to the resin) by applying HBTU (4 eq./building block), HOBt (4 eq./building block) and N,N-diisopropylethylamine (8 eq./building block) in NMP. The Fmoc-protecting groups were removed by using a solution

of 20% piperidine in NMP. The usual coupling reaction time was 1 h. The attachment of each amino acid residues was monitored by Kaiser-test [13] and by the detection of the cleaved Fmoc group at 290 nm in DMF. In the case of successful coupling the free residual amino nitrogens were acetylated with the mixture of acetic anhydride, dichloromethane and pyridine (10–80–10%). After the last coupling step the resin was rinsed by dichloromethane and methanol, and then it has been dried. Cleavage of the peptide from the resin was performed in the mixture of TFA, H₂O and triisopropylsilane (95–2.5–2.5%). The peptide was precipitated in diethyl ether, re-dissolved in water and freeze-dried. The crude product was purified by RP-HPLC (Shimadzu LC-20) using a Supelco Discovery BIO Wide Pore C18 (250×10 mm, 5 μm) semi preparative column. The compound was eluted by using the mixtures of water containing 0.1% TFA and acetonitrile (Eluent A: 100% H₂O, 0.1% TFA, Eluent B: 100% CH₃CN) with a 3mL/min flow rate and applying the following gradient program: 0-1 min 0 % B; 1-11 min 1 % B; 11-21 min 1-2 % B (linear gradient); 21-23 min 2-10 % B (linear gradient); 23-24 min 10 % B; 24-25 min 10-0 % B (linear gradient); 25-33 min 0 % B (R_t = 20.2 min). After purification the yield was 45.0%.

The peptide was identified by ESI-MS. The mass spectrometric measurements were obtained on a FinniganTSQ-7000 triple quadrupole mass spectrometer (Finnigan-MAT, San Jose, CA) equipped with a Finnigan electrospray ionization (ESI) source. The instrument was operated in positive ion mode, the ESI needle was adjusted to 4.5 kV and N₂ was used as a carrier gas. Analytical data: m/z = 986.5 [M + H]⁺, m/z = 493.8 [M + 2H]²⁺ and m/z = 329.3 [M + 3H]³⁺. The calculated monoisotopic molecular mass is: 985.48 Da. The ligand was obtained after purification as a trifluoroacetate salt. The HPLC chromatogram of the purified peptide is depicted in Fig. S1 (supporting information). The concentration of its stock solution was determined by potentiometric titrations. The purity was also confirmed by potentiometry and NMR.

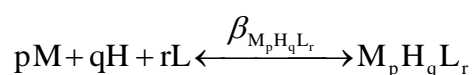
^1H NMR in D_2O , $\text{pH}^* = 7.0$, δ (in ppm): 1.26 (doublet (d), 3H, $^2\text{Ala-CH}_3$), 1.30 (multiplet (m), 2 \times 2H, $^{7,8}\text{Lys } \gamma\text{-CH}_2$), 1.63 (m, 2 \times 2H, $^{7,8}\text{Lys } \delta\text{-CH}_2$), 1.75 (m, 2 \times 2H, $^{7,8}\text{Lys } \beta\text{-CH}_2$), 2.54 (m, 2 \times 2H, $^{3,5}\text{Asp } \beta\text{-CH}_2$), 2.93 (m, 2 \times 2H, $^{7,8}\text{Lys } \varepsilon\text{-CH}_2$), 3.10 (m, 3 \times 2H, $^{1,4,6}\text{His } \beta\text{-CH}_2$), 3.99 (triplet (t), 1H, $^1\text{His } \alpha\text{-CH}$), 4.20 (m, 2 \times 1H, $^{7,8}\text{Lys } \alpha\text{-CH}$), 4.28 (quartet (q), 1H, $^2\text{Ala } \alpha\text{-CH}$), 4.49 (m, 2 \times 1H, $^{3,5}\text{Asp } \alpha\text{-CH}$), 4.51 (m, 2 \times 1H, $^{4,6}\text{His } \alpha\text{-CH}$), 6.92 and 6.99 (singlet and singlet (s and s), 1H and 1H, $^{4,6}\text{His } \text{C}^5\text{H}$), 7.03 (s, 1H, $^1\text{His } \text{C}^5\text{H}$), 7.81 and 7.88 (s and s, 1H and 1H, $^{4,6}\text{His } \text{C}^2\text{H}$), 7.84 (s, 1H, $^1\text{His } \text{C}^2\text{H}$).

2.2 Potentiometric measurements

The protonation and coordination equilibria were investigated by potentiometric titrations in aqueous solution ($I = 0.1 \text{ M NaCl}$, and $T = 298.0 \pm 0.1 \text{ K}$) under argon atmosphere, using an automatic titration set including a PC controlled Dosimat 665 (Metrohm) autoburette and an Orion 710A precision digital pH-meter. The Metrohm Micro pH glass electrode (125 mm) was calibrated [14] *via* the modified Nernst equation:

$$E = E_0 + K \cdot \log[\text{H}^+] + J_{\text{H}} \cdot [\text{H}^+] + \frac{J_{\text{OH}} \cdot K_{\text{w}}}{[\text{H}^+]}$$

where J_{H} and J_{OH} are fitting parameters in acidic and alkaline media for the correction of experimental errors, mainly due to the liquid junction and to the alkaline and acidic errors of the glass electrode; $K_{\text{w}} = 10^{-13.75} \text{ M}^2$ is the autoprotolysis constant of water [15]. The parameters were calculated by the non-linear least squares method. The complex formation was characterized by the following general equilibrium process:



$$\beta_{\text{M}_p\text{H}_q\text{L}_r} = \frac{[\text{M}_p\text{H}_q\text{L}_r]}{[\text{M}]^p[\text{H}]^q[\text{L}]^r}$$

where M denotes the metal ion and L the non-protonated ligand molecule. Charges are omitted for simplicity, but can be easily calculated taking into account the composition of the fully protonated peptide (H_8L^{6+}). The corresponding formation constants ($\beta_{M_pH_qL_r} \equiv \beta_{pqr}$) were calculated using the PSEQUAD computer program [16].

The protonation constants were determined from 4 independent titrations (90 data points per titration), with peptide concentration $1-1.5 \times 10^{-3}$ M. The complex formation constants were evaluated from 7 and 9 independent titrations (70-90 data points per titration) in case of the zinc(II) and copper(II) containing systems, respectively. The metal-to-ligand ratios were 2:1, 1:1 and 1:2 (in case of zinc(II) precipitation occurred above pH 7 at twofold metal ion excess). The metal ion concentrations varied between $0.6-2.9 \times 10^{-3}$ M. The titrations were performed between pH 2.6 and 11.4, but due to the rather low concentrations of the peptide ($-\log c_{\text{peptide}} = 2.5 - 3.2$), the derived equilibrium data of the processes below pH 3.6 and above pH 10.4 have increased uncertainties.

2.3 Electronic absorption and CD measurements

UV-Vis spectra were measured on a Unicam Helios α spectrophotometer using a cell with 1 cm optical pathlength. The CD spectra were recorded on a Jasco J-710 spectropolarimeter in the wavelength interval from 300 to 800 nm in a cell with 1 cm optical pathlength. The metal ion concentration was varied between $0.8-2.8 \times 10^{-3}$ M, depending on the metal-to-ligand ratio. For the copper(II) containing systems the pH-dependent UV-Vis spectra were treated together with pH-potentiometric data using the computer program PSEQUAD [16], resulting the formation constants (β_{pqr}) and the individual UV-Vis spectra of the copper(II) complexes. The individual CD spectra were also calculated by PSEQUAD.

2.4 EPR measurements

The EPR spectra were recorded at 77 K using a BRUKER EleXsys E500 spectrometer. All recorded EPR spectra in the systems were simulated with a spectrum decomposition method

by a computer program [17]. Since the copper(II) salt used to make the stock solution was a natural mixture of the isotopes, the spectrum of each species was calculated as the sum of spectra containing ^{63}Cu and ^{65}Cu weighted by their abundances in nature. The copper and ligand coupling constants are given in units of gauss (G); $1\text{ G} = 10^{-4}\text{ T}$.

NMR experiments – ^1H NMR measurements were performed on a Bruker Avance DRX 500 spectrometer. The spectra were recorded at $25\text{ }^\circ\text{C}$ in 100% D_2O solution, at a peptide concentration of $5 \times 10^{-3}\text{ M}$ (the tube diameter was 5 mm). The pH was adjusted to the desired values with NaOD. 2D COSY, TOCSY and ROESY spectra were acquired with $2048(\text{F}_2) \times 1024(\text{F}_1)$ complex points. The TOCSY experiments employed the MLEV17 sequence with a mixing time of 75 ms. ROESY spectra were acquired with mixing times of 300 ms. The chemical shifts δ were measured with respect to dioxane as internal reference and converted relative to SiMe_4 , using $\delta_{\text{dioxane}} = 3.70$. Data were processed using the Topspin 2.0 software package (Bruker).

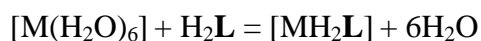
2.5 Determination of the superoxide dismutase activity

The SOD-like activity of the copper(II)-peptide complexes was studied at 298 K by using the indirect method of nitroblue tetrazolium (NBT) reduction [18]. The superoxide anion was generated *in situ* by the xanthine/xanthine oxidase reaction, and detected spectrophotometrically by monitoring the reduction of NBT at 560 nm. The reactions were carried out in a phosphate buffer ($5 \times 10^{-2}\text{ M}$), containing NBT ($5 \times 10^{-5}\text{ M}$) and xanthine ($1 \times 10^{-4}\text{ M}$). The reaction was initiated by adding an appropriate amount of xanthine oxidase to generate $\Delta A_{560} = 0.025\text{--}0.028\text{ min}^{-1}$. The NBT reduction rate was measured in the presence and absence of the investigated system ($[\text{Cu}^{2+}]_{\text{tot}} = 0\text{--}1 \times 10^{-6}\text{ M}$). In separate measurements, the activity of xanthine oxidase was monitored following the urate production by spectrophotometry at 298 nm, to rule out any inhibition induced by the copper(II)-L system. The SOD-like activity was

then expressed by the IC_{50} values (concentration that causes 50 % inhibition of NBT reduction).

2.6 Semiempirical quantum chemical calculations

In the MH_2L complexes the peptide may coordinate to the metal ion by six readily available binding sites (3 imidazole, 2 carboxylate and 1 amino group). To generate a set of inputs for the calculation, all possible coordination modes of the ligand were considered, with the following restriction: the binding terminal amino group, as the strongest donor site, was always included. Initial geometries of the complexes were generated and pre-optimized with molecular mechanics (using the keywords: UFF, BFGS line search, 0.1 gradient convergence, maximum 1000 steps) by the Arguslab computer program [19]. In the next step, a conformational search was performed by the computer program VegaZZ [20]. The SP4 force field and the AMMP-mom method were employed to assign charges. All flexible torsion angles were varied randomly. Dielectric constant was set to 78.4. For each initial geometry, 10000 conformers were generated and a 300 steps fast optimization was accomplished for each of them. For all considered coordination environment three conformers with the lowest energy were chosen for further optimization. Full geometry optimization was carried out with the PM6/EF/COSMO [21] semi empirical quantum chemical method, as implemented in MOPAC2009 [22] (with keywords PREC, NOMM, EPS=78.4 and UHF for Cu(II) and RHF for Zn(II)). The convergence criterion was typically a gradient norm of 1 kcal/mol (4.18 kJ/mol). We use kcal in this article, because it is conventional in theoretical chemistry. For Cu(II)-complexes, the lowest energy structures were accepted when the relation $0,75 < S^2 < 1$ was satisfied, otherwise the next best structure from the conformational search has been optimized. From the converged MOPAC output the standard molar enthalpy of formation ($\Delta_f H_m^\circ$) was extracted, from which the standard molar enthalpy of reaction was calculated according to the following equation:



($\Delta_r H_m^\circ = \Delta_f H_m^\circ([MH_2L]) + 6 \times \Delta_f H_m^\circ(H_2O) - (\Delta_f H_m^\circ(H_2L) + \Delta_f H_m^\circ([M(H_2O)_6]))$), where M is either Cu(II) or Zn(II). The following standard molar enthalpy of formation were used: $\Delta_f H_m^\circ(H_2O) = -68.3$ kcal/mol, $\Delta_f H_m^\circ(Cu(H_2O)_6)^{2+} = 15.5$ kcal/mol, $\Delta_f H_m^\circ(Zn(H_2O)_6)^{2+} = -36.6$ kcal/mol [23], while $\Delta_f H_m^\circ(H_2L) = -627.1$ kcal/mol was calculated by MOPAC2009 for the relaxed peptide. Since during the calculation only implicit water environment has been considered, the calculated $\Delta_r H_m^\circ$ values are comparable with each other, but may differ considerably from the experimental values.

3. Results and discussion

There is a discrepancy in the literature concerning the exact sequence of the N-terminal part of the Cu,Zn SOD of *A. pleuropneumoniae*. Earlier isolation of the enzyme was based on cloning of *sodC* of *A. pleuropneumoniae*, encoding the enzyme in question [24]. The primary gene product was shown to have a leader peptide at the N-terminus (¹MKLTNLALAF¹¹TLFGASAVAF²¹AHADHDHKKK³¹DNSAVEKLVV ...). Originally, the leader peptide peptidase cleavage site was suggested after the 23th amino acid [24]. Later, the cleavage site between the positions 21 and 22 has been proposed [8]. Unfortunately, the protein used to prepare single crystals [25] lacks the whole N-terminal domain and starts only from ²⁹K. However, the location of signal peptidase cut can be determined with very good reliability using the SignalP 3.0 server [26], which predicts the cleavage site, with 0.889 probabilities, between positions 21 and 22. Therefore, it is highly probable that the N-terminal eight amino acids of *A. pleuropneumoniae* Cu,Zn SOD is HADHDHKK. On the other hand, from a biological point of view, it makes sense that this enzyme has a similar HxDHxH-type N-terminal metal binding site to those from haemophilus species [8,11].

3.1 Protonation of the ligand. The studied octapeptide undergoes 8 (de)protonation processes between pH 2-12. The first two deprotonation constants (pK_1 and pK_2 , Table 1) belong to the Asp carboxylates. The pK s related to the imidazole rings and the N-terminal amino group are in the range generally observed for His-containing peptides ($pK_{3,4,5} = 5.19 - 6.65$, $pK_6 = 7.55$, Table 1). Above pH 10 the deprotonation of the two lysine ϵ - NH_3^+ take place, in an overlapping manner. Due to the relatively low peptide concentration applied in our measurements the $pK < 3.6$ and $pK > 10.4$ values have somewhat higher uncertainties than usual for pH-potentiometric studies (see also the experimental part).

3.2 Zinc(II) complexes. In equimolar solutions of zinc(II) and **L** seven differently protonated complexes were detected between pH 3 and 11.4 (Fig. 1.). The peptide has six readily available binding sites for zinc(II) (3 imidazole, 2 carboxylate and 1 amino groups). The 1N and 2N coordinated ZnH_4L and ZnH_3L complexes formed in the acidic pH-region are most probably present in form of binding/protonation isomers, with the possible additional coordination of carboxylate groups. The two protons in the complex ZnH_2L , being dominant around pH 7, are very likely located on the non-coordinating lysine ϵ -amino groups. Peptides with an unprotected N-terminal histidine favor the histamine-like $\{NH_2, N_{im}\}$ coordination to zinc(II) [27-29]. However, the equilibrium constant of the process $Zn^{2+} + H_2L = ZnH_2L$ ($\log K = 6.58$) is higher than the related value for histamine itself ($\log \beta_{101} = 5.15$ [30]), or those of some $\{3N_{im}\}$ and $\{NH_2, 2N_{im}\}$ coordinated complexes ($\log K = 5.1$ [31] and 5.94 [29], respectively), indicating that additional binding sites should be taken into consideration. Therefore 1H NMR investigations have been performed to identify the metal binding sites in ZnH_2L . The assignment of the proton signals was based on COSY and TOCSY experiments. The differentiation of the signals related to $^3Asp/^5Asp$ and $^7Lys/^8Lys$ was not possible under our experimental conditions, due to their very similar and overlapping resonances. Similarly, only the N-terminal histidine (1His) signals can be distinguished from the three histidine units.

The changes of the ^1H NMR spectra upon addition of zinc(II) are depicted in Fig. 2. The $^7\text{Lys}/^8\text{Lys}$ signals are not affected by the zinc(II) coordination confirming that the two lysine ϵ -amino groups are protonated in ZnH_2L . In spite of that, the CH_α signal of the terminal ^1His shows notable shift (~ 0.2 ppm) and broadening with increasing zinc(II) concentration, which supports its histamine-like coordination. However, apart from the lysine (and dioxane) resonances, all other signals are more or less broadened upon zinc(II) coordination, therefore the effect is not site-selective. Nevertheless, the extent of shift and broadening is different for the different residues, which provides some further information. Among the histidine aromatic signals, one of the two non-terminal C2H/C5H pairs is much less affected than the other two. Moreover, the Asp- CH_2 signals become asymmetric (and broadened) upon zinc coordination. These observations suggest $\{\text{NH}_2, 2\text{N}_{\text{im}}, \text{COO}^-_{\text{Asp}}\}$ donor set around the metal ion in ZnH_2L , although the formation of binding isomers in lower concentrations cannot be excluded definitely. Indeed, the twelve most stable structures resulted by the semiempirical calculations have $\{\text{NH}_2, 2\text{N}_{\text{im}}, \text{COO}^-_{\text{Asp}}\}$ donor set, but all the three His and both Asp may participate in the coordination (see later). It is noteworthy, that this species has more than two log units lower stability than the corresponding complex of the N-terminal fragment of *H. ducreyi* Cu,ZnSOD ($\log K = 8.93$), where $\{\text{NH}_2, 3\text{N}_{\text{im}}, \text{S}_{\text{Met}}, \text{COO}^-_{\text{Asp}}\}$ donor set has been determined [12].

Increasing the pH above 7, the complex ZnH_2L releases four additional protons with $\text{pK} = 8.07, 9.16, 10.25$ and 11.2 , respectively. Two of them are related to the deprotonation of lysine $\epsilon\text{-NH}_3^+$, while the other two belong either to the formation of mixed hydroxo complexes or to metal promoted deprotonations of amide nitrogens. In order to determine the metal binding sites in ZnHL, NMR investigations have been performed at pH 8.5, too. The spectral features (Fig. S2, supporting information) are very similar to those observed at pH 7 (Fig. 2). New peaks reflecting slow exchange between the free and bound ligand, observed

earlier for amide-coordinated zinc(II) complexes of Gly-His, Ala-His and Gly-His-Lys [32,33], were not detected, suggesting that zinc(II) promoted deprotonation of amide nitrogen(s) is unlikely at pH 8.5. Moreover, the peaks related to $^7\text{Lys}/^8\text{Lys}$ are unchanged upon zinc(II) binding, indicating that these residues are still protonated. Consequently, the first (and probably the second) deprotonation(s) are related to the formation of mixed hydroxo complexes ($\text{ZnHL}=\text{Zn}(\text{H}_2\text{L})\text{OH}$ and $\text{ZnL}=\text{Zn}(\text{H}_2\text{L})(\text{OH})_2$), similarly to many other zinc(II)-peptide systems [12,34]. Therefore, during the last two processes the deprotonation of the Lys residues take place. Indeed, the observed pKs (10.25, 11.2) are close to those of the lysine residues in the absence of zinc(II).

At two-fold excess of ligand over the metal ion *bis*-complexes ($\text{Zn}(\text{H}_3\text{L})_2$, $\text{Zn}(\text{H}_3\text{L})(\text{H}_2\text{L})$ and $\text{Zn}(\text{H}_2\text{L})_2$) are also formed between pH 5.0 and 9.5. Such complexes of peptides with unprotected N-terminal histidine generally have *bis*-histamine $\{2\text{NH}_2, 2\text{N}_{\text{im}}\}$ type binding [27-29], which provides relatively high stability (*e.g.* $\log K = 10.05$ in the case of HVGD peptide [28]). In the present case the equilibrium constant of the analogous process $\text{Zn}^{2+} + 2\text{H}_2\text{L} = \text{Zn}(\text{H}_2\text{L})_2$ is rather similar ($\log K = 10.27$), although considering the size difference between the two peptide, the somewhat higher $\log K$ value may suggest additional $\text{N}_{\text{im}}/\text{COO}^-$ coordination beside the *bis*-histamine type binding.

3.3 Copper(II) complexes. The copper(II) binding ability of **L** has been studied by combined pH-metric, UV-Vis, CD and EPR spectroscopic methods. The octapeptide **L** forms water soluble complexes over the whole pH range studied, even at twofold metal ion excess. The pH dependent UV-Vis and CD spectra obtained at different metal-to-ligand ratios show continuous shift between pH 3 and 11 (Figs. 3 and 4), indicating the subsequent formation of several complexes with different protonation states. The comparative evaluation of pH-metric, UV-Vis and CD spectroscopic results indicated the formation of 9 mononuclear and 6 dinuclear species (Table 1, Fig. 5). Except CuH_4L , under appropriate conditions the

concentration all these species are $> 0.3[\text{Cu}^{\text{II}}]_{\text{TOT}}$, which allowed us to determine their individual UV-Vis and CD spectra (Figs. S3 and S4, supporting information). These individual spectra, complemented by the EPR study performed at 77 K (Fig. 6), were used to derive information on the formed complexes.

In equimolar solution of copper(II) and **L** protonated CuH_5L , CuH_4L , CuH_3L and CuH_2L complexes are formed between pH 3 and 7 (Fig. 5.A). The individual electronic absorption spectra of these species (Fig. S3.A) show increasing number of nitrogen donors of copper(II). The low intensity CD spectra (Fig. S4.A) in the amide region (300-400 nm) indicate the coordination of only side chain donors (N-terminal amino, imidazole or carboxylate groups) creating macrochelates around the metal ion. The low pKs of the processes leading to these species ($\text{CuH}_5\text{L} = \text{CuH}_4\text{L} + \text{H}^+$, pK = 3.96; $\text{CuH}_4\text{L} = \text{CuH}_3\text{L} + \text{H}^+$, pK = 3.6) together with the spectral data (Table 2) suggest 1N, 2N and 3N coordination in CuH_5L , CuH_4L and CuH_3L , respectively. Between pH 6 and 8 CuH_2L is the dominant species (Fig. 5.A), in which the two protonated lysine ϵ -amino groups are protonated, similarly to ZnH_2L . The EPR parameters determined for this species (Table 2) indicate the coordination of four non-amide nitrogen to the metal ion. Indeed, the pK of its formation ($\text{CuH}_3\text{L} = \text{CuH}_2\text{L} + \text{H}^+$, pK = 5.06) is lower than the pKs of the imidazole rings and N-terminal amino group in the absence of metal ion (pK_{3,4,5} = 5.2 – 6.7, pK₆ = 7.55, Table 1), indicating their involvement in the metal ion binding. The thermodynamic stability of this species ($\text{Cu}^{2+} + \text{H}_2\text{L} = \text{CuH}_2\text{L}$, log K = 12.68) is much higher than that reported for the $\{\text{NH}_2, 2\text{N}_{\text{im}}\}$ coordinated Cu^{2+} -HVH (log K = 10.53, [28]), or for the $\{4\text{N}_{\text{im}}\}$ coordinated Cu^{2+} -cyclo-(GH)₄ complex (log K = 9.35, [35]). Consequently, the metal binding sites in CuH_2L involve the N-terminal amino group and the three imidazole rings, which create two macrochelates in the equatorial plane of the metal ion. This coordination mode has been also suggested by the semiempirical calculations (see later). However, similar $\{\text{NH}_2, 3\text{N}_{\text{im}}\}$ coordination environment, but somewhat lower stability (Cu^{2+}

+ HL = CuHL, log K = 11.73 [12]) has been detected for the analogous copper(II) complex of the N-terminal peptide of *H. ducreyi* Cu,Zn SOD. Since the UV-Vis and EPR parameters of the two complexes are very similar, the higher stability of the presently studied complex is probably due to a more favorable conformation of the peptide. Interestingly, the extremely high stability of CuH₂L is achieved by side chain donors only, *i.e.* the coordination of backbone amide nitrogen(s), frequently observed in the copper(II)-peptide systems already at pH 4-6, does not occur in CuH₂L.

At higher pH two strongly overlapped deprotonations have been detected resulting in the formation of CuL. The electronic absorption and CD spectra (Figs. 3 and 4) are strongly blue shifted during these processes. The spectral parameters obtained for CuL (Table 2) indicate notably increased equatorial ligand field around the metal ion. All these facts are compatible with the successive deprotonation and coordination of two adjoining amide nitrogens. The octapeptide L has two major metal binding sites which involve two amide nitrogens: the N-terminal ¹HAD residue with {NH₂,2N⁻,COO⁻}, and the ⁴HDH moiety with {N_{im},2N⁻,N_{im}} type binding modes. However, strongly overlapped deprotonations are characteristic only for the latter one [36-38], since the proton loss of the second amide nitrogen in the first formed {N_{im},N⁻,N_{im}} coordinated species is a very favorable process. Up to pH 11 two further, overlapped deprotonations have been observed. The electronic absorption and CD spectra of CuH₋₁L and CuH₋₂L are nearly identical with those of the former species CuL (Figs. S3 and S4), suggesting the deprotonation of a lysine ε-NH₃⁺ group in these processes (pK = 10.01 and 10.79).

Above pH 11 important changes have been observed both in the visible and CD spectra (Figs. 3 and 4), which reflects the coordination of a third amide nitrogen, since only these donor groups may transmit strong chiral perturbation to the copper(II). Consequently, the metal ion possesses either {NH₂,3N⁻} or {3N⁻,N_{im}} type coordination in CuH₋₃L. Although, the

spectral data clearly indicate the formation of this species, due to the high pH and the low ligand concentration used (see also the experimental part), the corresponding $\log \beta_{1-31}$ value is rather uncertain.

At twofold metal ion excess dinuclear complexes are formed, similarly to other multihistidine peptides [12,39]. The UV-Vis, CD and EPR spectra recorded as a function of pH reflect again increasing number of nitrogen donors around the metal ions with increasing pH. Although, the extremely high stability of CuH_2L resulted from the coordination of only side chain donors, they can not provide high affinity binding for two copper ions. Therefore, the first dinuclear complex (Cu_2HL) formed around pH 5-6 already contains coordinated amide nitrogen(s), as reflected by intense CD spectra especially in the UV region (Figs. 4 and S4). The successive formations of the complexes Cu_2HL , Cu_2L and $\text{Cu}_2\text{H}_{-1}\text{L}$ are strongly overlapped (Fig. 5.B). Although the visible and CD spectra show important changes between pH 5-7, their EPR spectra can be only described by a common broad singlet, due to the interacting copper(II) centers. Considering that several isomers can be expected for these species, clear binding site assignment cannot be made. In contrast with these complexes, $\text{Cu}_2\text{H}_{-2}\text{L}$ is a major species between pH 8-9. During its formation considerable spectral change can be observed, indicating the deprotonation and coordination of a further amide nitrogen. Since in this species the lysine ϵ -amino groups are still protonated, two amide nitrogens are bound to each metal ions, which may explain their high stability. Surprisingly, relatively well resolved EPR spectra can be obtained between pH 8-9 at two fold metal ion excess (Fig. 6.B). The evaluation of these spectra indicates the presence of two separated copper(II) centers with different coordination environments (Table 2). This is also supported by the unusual CD spectrum of all dinuclear species, containing two positive CD bands at 500 and 610 (710) nm (Fig. S4.B). Considering the major binding sites of the ligands, the metal ions in $\text{Cu}_2\text{H}_{-2}\text{L}$ have $\{\text{NH}_2, 2\text{N}^-, \text{COO}^-\}$ and $\{\text{N}_{\text{im}}, 2\text{N}^-, \text{N}_{\text{im}}\}$ type coordination. During the

next two deprotonations the spectral parameters are practically unchanged, indicating identical coordination environment around the metal ions. Consequently the deprotonations of the lysine $\epsilon\text{-NH}_3^+$ groups take place in these processes. On the other hand, the last deprotonation observed ($\text{Cu}_2\text{H}_4\text{L} = \text{Cu}_2\text{H}_5\text{L} + \text{H}^+$, $\text{pK} = 11.34$) results in an important spectral change again, indicating the coordination of a further amide nitrogen to one of the copper(II) centers.

3.4 Metal sequestering properties. Considering only the non-amide bounded species (in fact the amide coordination is very rare in biological systems), to our knowledge **L** is the strongest copper(II) chelator at pH 7.4 among the oligopeptides studied so far. Its copper(II) binding ability is even higher than that of the recently reported N-terminal sequence of *H. ducreyi* Cu,Zn SOD [11]. This can be also demonstrated by calculating the apparent (conditional) dissociation constant (K_D) at pH 7.4 and 1:1 metal-to-ligand ratio,

$$\text{MH}_x\text{L} = \text{H}_x\text{L} + \text{M}^{2+}_{\text{free}}, \quad K_{D,M} = [\text{H}_x\text{L}][\text{M}^{2+}_{\text{free}}]/[\text{MH}_x\text{L}]$$

where H_xL and MH_xL denote the total concentration of the free peptide and complexes, respectively, including all possible protonation states. Based on the equilibrium data listed in Table 1, $K_{D,\text{Cu}} = 7.4 \times 10^{-13}$ M can be calculated. This extraordinary sequestering capacity supports copper(II) chaperoning role of the N-terminal His-rich region of Gram-negative bacteria, already assumed for *H. ducreyi* Cu,Zn SOD [11,12]. On the other hand, the zinc(II) binding ability of this peptide is relatively modest ($K_{D,\text{Zn}} = 4.8 \times 10^{-7}$ M), it is ~ 2.5 order of magnitudes lower than that determined for the N-terminal sequence of *H. ducreyi* Cu,Zn SOD ($K_{D,\text{Zn}} = 1.6 \times 10^{-9}$ M [12]). Consequently, the present data do not confirm the role of N-terminal His-rich region in zinc(II) sequestering over the Gram-negative bacteria, which was originally suspected based on the high affinity zinc(II) binding reported in [12].

3.5 SOD-like activity of the copper(II)-peptide system. The SOD-like activity of the copper(II)-**L** system was tested indirectly, by its ability to inhibit the reaction between the O_2^- radical and NBT (Fig. 7). Although this method has some drawbacks [40], it is very commonly used, and therefore allows a comparison with a number of similar systems. The determined IC_{50} values are listed in Table 3, together with those of some highly active histidine-based SOD mimics, taken from the literature. Although the activity of the copper(II)-**L** complexes at pH 7 is *c.a.* 24-fold lower than that of the native Cu,Zn SOD enzyme from bovine liver, it is one of the most active peptide complex reported so far. The correct interpretation of the observed SOD-like activity requires the knowledge of speciation in the rather diluted solutions used ($[Cu^{2+}]_{tot} = [L]_{tot} \sim 0.1 \mu M$). Even under this condition, the complex CuH_2L is the dominant species (97%) at pH 7, while the free metal ion represents only 0.3 % of the total copper(II) concentration. Consequently, the observed SOD-like activity is related to the species CuH_2L . Table 3 lists the most active peptide complexes reported so far, and a survey of the listed ligands may support the general view, that macrochelated multiimidazole coordination around copper(II) results in very efficient SOD-like activity [41,42]. Such coordination is probably favored by copper(I), and thus facilitate the redox cycling between copper(II) and copper(I).

The observed high activity further supports our earlier speculation on the multifunctional role of the copper(II)-bound N-terminal His-rich domain of Cu,Zn SODs of some Gram-negative bacteria [12], *i.e.* beside the chaperoning role it may also behave as a temporary (low activity) superoxide dismutating center in the case of copper(II) affluence of bacterial periplasm.

3.6 Semiempirical quantum chemical calculations. The results of the calculations for the MH_2L complexes ($M = Zn(II)$ and $Cu(II)$) are summarized in the Table S1 (supporting information). In the case of ZnH_2L the first twelve most stable structures have $\{NH_2, 2N_{im}, COO^-_{Asp}\}$ donor set, and the first five involve the stable histamine-like chelate

coordination of the N-terminal His residue. These results are in excellent agreement with the experimental data presented above. The two most stable structures are depicted in Fig. 8.A and Fig. S6.A (supporting information), respectively.

Among the five most stable structures for CuH_2L three have $\{\text{NH}_2, 3\text{N}_{\text{im}}\}$ donor set (Table S1), also suggested by the experimental data. However, the first and third most stable structures possess $\{\text{NH}_2, 2\text{N}_{\text{im}}, \text{COO}^-_{\text{Asp}}\}$ coordination environment with bidentate carboxylate coordination in the equatorial plane of copper(II), resulting in a strongly distorted seven-coordinated geometry around the metal ion (Fig. S6.B). Since, this coordination mode is rather unusual and is inconsistent with the experimental findings, the corresponding structures have been rejected. The remaining three among the five most stable structures, having $\{\text{NH}_2, 3\text{N}_{\text{im}}\}$ donor set with the participation of all the three His units, are conformational isomers. The two most stable accepted structures are depicted in Fig. 8.B and Fig. S6.C (supporting information), respectively.

4. Conclusion

The N-terminal octapeptide of *A. pleuropneumoniae* Cu,ZnSOD ($\text{H}_2\text{N-HADHDHKK-OH}$, **L**) has highly versatile metal binding ability, it provides two high affinity binding sites for copper(II). In equimolar solutions the MH_2L complexes ($\text{M} = \text{Cu(II)}, \text{Zn(II)}$) are dominant in the neutral pH-range. **L** has extraordinary copper(II) sequestering capacity ($K_{\text{D,Cu}} = 7.4 \times 10^{-13}$ M at pH 7.4), which is provided only by side chain donors. The central ion in CuH_2L is coordinated by four nitrogens $\{\text{NH}_2, 3\text{N}_{\text{im}}\}$ in its equatorial plane. In ZnH_2L the peptide binds to zinc(II) through a $\{\text{NH}_2, 2\text{N}_{\text{im}}, \text{COO}^-\}$ donor set, providing a relatively modest zinc binding affinity ($K_{\text{D,Zn}} = 4.8 \times 10^{-7}$ M at pH 7.4). Consequently, the presented data do support a general chaperoning role of the N-terminal His-rich region of Gram-negative bacteria in copper(II)

uptake, but do not confirm similar function for zinc(II). The proposed structure for the MH_2L complexes have been verified by semiempirical quantum chemical calculations, too.

Interestingly, the CuH_2L has very important SOD-like activity, which may allow to speculate on the multifunctional role of the copper(II)-bound N-terminal His-rich domain of Cu,Zn SODs of Gram-negative bacteria.

5. Abbreviations:

SOD: Superoxide dismutase

ESI-MS: Electrospray ionization mass spectrometry

COSY: Correlation spectroscopy

TOCSY: Total correlation spectroscopy

ROESY: Rotational frame Overhauser effect spectroscopy

CD: Circular dichroism

DMF: Dimethylformamide

TFA: Trifluoroacetic acid.

Appendix A. Supplementary data

Supplementary data (HPLC chromatogram of the purified peptide, 1H NMR spectra of **L** in D_2O ($T = 298$ K) as a function of increasing zinc(II) concentration at pH* 8.5, individual UV-Vis, CD and anisotropic EPR spectra of some major copper(II)-**L** complexes, and some calculated structures) associated with this article can be found in the online version, at doi:???

Acknowledgements

This work was supported by the Hungarian Scientific Research Found (OTKA K63606) and TÁMOP 4.2.1/B-09/1/KONV-2010-0005.

References

- [1] J.V. Bannister, W.H. Bannister, G. Rotilio, *CRC Crit. Rev. Biochem.* 22 (1987) 111-180.
- [2] A. Battistoni, *Biochem. Soc. Trans.* 31 (2003) 1326-1329.
- [3] A. Pesce, C. Capasso, A. Battistoni, S. Folcarelli, G. Rotilio, A. Desideri, M. Bolognesi, *J. Mol. Biol.* 274 (1997) 408-420.
- [4] D. Bordo, A. Pesce, M. Bolognesi, M.E. Stroppolo, M. Falconi, A. Desideri, in: A. Messerschmidt, R. Huber, T. Poulos, K. Wieghardt, (Eds.), *Handbook of Metalloproteins*, John Wiley and Sons, Ltd, Chichester, 2001, pp. 1284-1300.
- [5] J.S. Kroll, P.R. Langford, B.M. Loynds, *J. Bacteriol.* 173 (1992) 7449-7457.
- [6] H.M. Steinman, *J. Biol. Chem.* 257 (1982) 10283-10293.
- [7] L. Spagnolo, I. Toro, M. D'Orazio, P. O'Neill, J.Z. Pedersen, O. Carugo, G. Rotilio, A. Battistoni, K. Djinovic-Carugo, *J. Biol. Chem.* 279 (2004) 33447-33455
- [8] A. Battistoni, F. Pacello, A.P. Mazzetti, C. Capo, S.J. Kroll, P. Langford, A. Sansone, G. Donnarumma, P. Valenti, G. Rotilio, *J. Biol. Chem.* 276 (2001) 30315-30325.
- [9] U.E. Schaible, S.H. Kaufmann, *Trends Microbiol.* 13 (2005) 373-380.
- [10] C. Harford, B. Sarkar, *Acc. Chem. Res.* 1997, 30, 123-130
- [11] P. D'Angelo, F. Pacello, G. Mancini, O. Proux, J.L. Hazemann, A. Desideri, A. Battistoni, *Biochemistry* 44 (2005) 13144-13150.
- [12] Z. Paksi, A. Jancsó, F. Pacello, N.V. Nagy, A. Battistoni, T. Gajda, *J. Inorg. Biochem.* **102**, 1700-1710, 2008.
- [13] E. Kaiser, R.L. Colescott, C.D. Bossinger, P.I. Cook, *Anal. Biochem.* 34 (1970) 595-598.
- [14] F.J.C. Rosotti, H. Rosotti, *The determination of stability constants*, McGraw-Hill Book Co., New York, 1962, p. 149.

- [15] E. Högfeldt, *Stability Constants of Metal-Ion Complexes, Part A. Inorganic Ligands*, Pergamon, New York, 1982, p. 32.
- [16] L. Zékány, I. Nagypál, G. Peintler, *PSEQUAD for chemical equilibria*, Technical Software Distributors: Baltimore, MD, 1991.
- [17] A. Rockenbauer, L. Korecz, *Appl. Magn. Reson.* 10 (1996) 29-43
- [18] C. Beauchamp, I. Fridovich, *Anal. Biochem.* 44 (1971) 276–287.
- [19] ArgusLab 4.0.1, Mark A. Thompson, Planaria Software LLC, Seattle, WA,
<http://www.arguslab.com>
- [20] A. Pedretti G. Vistoli, *VEGA ZZ* (1996–2010), <http://www.ddl.unimi.it/vega/>
- [21] J.P. James, *J. Mol. Model.*, 13, (2007) 1173-1213.
- [22] MOPAC2009, Version 9.0*, J.J.P. Stewart (2009), <http://OpenMOPAC.net>
- [23] J.D. Cox, D.D. Wagman, V.A. Medvedev, *CODATA Key Values for Thermodynamics*, Hemisphere Publ. Corp., New York (1989).
- [24] P.R. Langford, B.M. Loynds, J. S. Kroll, *Infect. Immun.* 64 (1996) 5035-41.
- [25] K.T. Forest, P.R. Langford, J.S. Kroll, E.D. Getzoff, *J. Mol. Biol.*, 296 (2000) 145-153.
- [26] J.D. Bendtsen, H. Nielsen, G. von Heijne, S. Brunak, *J. Mol. Biol.*, 340 (2004) 783-795,
Improved prediction of signal peptides: SignalP 3.0., <http://www.cbs.dtu.dk/services/SignalP/>
- [27] I. Sóvágó, in: K. Burger (Ed.), *Biocoordination Chemistry*, Ellis Horwood, Chichester, 1990, pp 135-184.
- [28] A. Myari, G. Malandrinos, Y. Deligiannakis, J. Plakatouras, N. Hadjialidis, Z. Nagy, I. Sóvágó, *J. Inorg. Biochem.* 85 (2001) 253-261.
- [29] A. Myari, G. Malandrinos, J. Plakatouras, N. Hadjialidis, I. Sóvágó, *Bioinorg. Chem. Appl.* 1 (2003) 99-112.

- [30] I. Török, T. Gajda, B. Gyurcsik, G.K. Tóth, A. Péter, *J. Chem. Soc., Dalton Trans.* (1998) 1205-1212.
- [31] A. Jancsó, Z. Paksi, N. Jakab, B. Gyurcsik, A. Rockenbauer, T. Gajda, *Dalton Trans.* (2005) 3187-3194.
- [32] S.A. Daignault, A.P. Arnold, A.A. Isab, D.L. Rabenstein, *Inorg. Chem.* 24 (1985) 3984-3988.
- [33] D.L. Rabenstein, S.A. Daignault, A.A. Isab, A.P. Arnold, M.M. Shoukry, *J. Am. Chem. Soc.* 107 (1985) 6435-6439.
- [34] M. Mylonas, A. Krzel, J.C. Plakatouras, N. Hadjiliadis, W. Bal, *Bioinorg. Chem. Appl.* 2 (2004) 125-140.
- [35] R. Bonomo, G. Impellizzeri, G. Pappalardo, R. Purrello, E. Rizzarelli and G. Tabbi, *J. Chem. Soc., Dalton Trans.* (1998) 3851-3857.
- [36] D. Valensin, F.M. Mancini, M. Luczkowski, A. Janicka, K. Wisniewska, E. Gaggelli, G. Valensin, L. Lankiewicz, H. Kozlowski, *J. Chem. Soc. Dalton Trans.*, 2004, 16.
- [37] B. Bóka, A. Myari, I. Sóvágó, N. Hadjialidis, *J. Inorg. Biochem.*, 98 (2004) 113-122.
- [38] M. Casoralo, M. Chelli, M. Ginanneschi, F. Laschi, M. Muniz-Miranda, A.M. Papini, G. Sbrana *Spectrochim. Acta.* 1999, **55A**, 1675-1689.
- [39] D. Vaslensin, L. Szyrwił, F. Camponeschi, M. Rowinska-Zyrek, E. Molteni, E. Jankowska, A. Szymanska, E. Gaggelli, G. Valensin, H. Kozlowski, *Inorg. Chem.* 48 (2009) 7330-7340.
- [40] O. Iranzo, *Bioorg. Chem.* 39 (2011) 73-87.
- [41] S. Timári, R. Cerea, K. Várnagy, *J. Inorg. Biochem.* 105 (2011) 1009-1017.
- [42] P. Stanczak, H. Kozlowski, *Biochem. Biophys. Res. Comm.* 352 (2007) 198–202.
- [43] B. Bóka, A. Myari, I. Sóvágó, N. Hadjiliadis, *J. Inorg. Biochem.* 98 (2004) 113-122.

- [44] R.P. Bonomo, V. Bruno, E. Conte, G. De Guido, D. La Mendola, G. Maccarone, F. Nicoletti, E. Rizzarelli, S. Sortino, G. Vecchio, Dalton Trans. (2003) 4406-4415.

Table 1. Formation constants of the proton, zinc(II) and copper(II) complexes of NH₂-HADHDHKK-OH (estimated errors in parentheses (last digit)) (*I* = 0.1 M NaCl, *T* = 298 K).

H_qL_r	pqr	log β_{pqr}	pK		
HL	011	10.8(2)	10.8		
H ₂ L	021	20.96(8)	10.16		
H ₃ L	031	28.51(1)	7.55		
H ₄ L	041	35.16(1)	6.65		
H ₅ L	051	41.18(1)	6.02		
H ₆ L	061	46.37(1)	5.19		
H ₇ L	071	49.96(8)	3.59		
H ₇ L	071	52.7(2)	2.7		
M_pH_qL_r	pqr	log β_{pqr}	pK/log K	log β_{pqr}	pK/log K
			M = Zn(II)		M = Cu(II)
MH ₅ L	151	–		46.29(8)	pK = 3.99
MH ₄ L	141	38.76(7)	pK = 5.25	42.3(1)	pK = 3.6
MH ₃ L	131	33.51(4)	pK = 5.97	38.71(6)	pK = 5.06
MH ₂ L	121	27.54(3)	log K = 6.58, pK = 8.07	33.66(2)	log K = 12.70
MHL	111	19.47(3)	pK = 9.16	–	
ML	101	10.31(3)	pK = 10.26	17.17(4)	pK = 10.01
MH ₁ L	1–11	0.05(3)	pK = 11.19	7.16(4)	pK = 10.79
MH ₂ L	1–21	–11.14(4)	–	–3.63(4)	(pK = 12.0)
MH ₃ L	1–31	–		[–15.6(4)]	–
MH ₆ L ₂	142	66.0(1)	pK = 6.80	–	
MH ₅ L ₂	132	59.2(1)	pK = 7.01	–	
MH ₄ L ₂	122	52.19(6)	log K = 10.27	57.73(6)	log K = 15.81
M ₂ HL	211	–		30.93(1)	pK = 5.67
M ₂ L	201	–		25.25(3)	pK = 6.71
M ₂ H ₁ L	2–11	–		18.54(5)	pK = 7.43
M ₂ H ₂ L	2–21	–		11.11(1)	pK = 9.60
M ₂ H ₃ L	2–31	–		1.51(3)	pK = 10.71
M ₂ H ₄ L	2–41	–		–9.20(1)	pK = 11.31
M ₂ H ₅ L	2–51	–		–20.51(8)	

Table 2. Parameters of the d-d transitions and anisotropic EPR spectra^a of the components obtained in the Cu(II) – L system, and the proposed coordination mode in the equatorial plane of copper(II)

Species	$\lambda^{\text{d-d}}_{\text{max}}$ (nm)	g_{xx}	g_{yy}	g_{zz}	A_{xx}/G	A_{yy}/G	A_{zz}/G	Coordination mode
Cu(II)	~ 820	2.081	2.424	10.8	110.0			
CuH ₅ L ^b	680	2.063	2.268	15.0	164.0			
CuH ₄ L ^b	–	2.063	2.268	15.0	164.0			
CuH ₃ L ^b	645	2.063	2.268	15.0	164.0			NH ₂ ,2N _{im}
CuH ₂ L	595	2.050	2.238	21.4	181.0			NH ₂ ,3N _{im}
CuL ^c	545	2.045	2.034	2.201	26.7	24.7	195.9	N _{im} ,N ⁻ ,N ⁻ ,N _{im}
CuH ₁ L ^c	550	2.045	2.034	2.201	26.7	24.7	195.9	N _{im} ,N ⁻ ,N ⁻ ,N _{im}
CuH ₂ L ^c	545	2.045	2.034	2.201	26.7	24.7	195.9	N _{im} ,N ⁻ ,N ⁻ ,N _{im}
CuH ₃ L	510							N _{im} ,N ⁻ ,N ⁻ ,N ⁻
CuH ₄ L ₂	610							
Cu ₂ HL ^d	680	2.118	2.118	63.0	63.0			^e
Cu ₂ L ^d	595	2.118	2.118	63.0	63.0			^e
Cu ₂ H ₁ L ^d	590	2.118	2.118	63.0	63.0			^e
Cu ₂ H ₂ L ^f comp.1	550	2.050	2.250	21.0	183.0			NH ₂ ,2N ⁻ ,O ⁻
comp.2		2.045	2.170	30.2	185.0			N _{im} ,2N ⁻ ,N _{im}
Cu ₂ H ₃ L ^f comp.1	550	2.050	2.250	21.0	183.0			NH ₂ ,2N ⁻ ,O ⁻
comp.2		2.045	2.170	30.2	185.0			N _{im} ,2N ⁻ ,N _{im}
Cu ₂ H ₄ L ^f comp.1	550	2.050	2.250	21.0	183.0			NH ₂ ,2N ⁻ ,O ⁻
comp.2		2.045	2.170	30.2	185.0			N _{im} ,2N ⁻ ,N _{im}
Cu ₂ H ₅ L	530							NH ₂ ,3N ⁻ N _{im} ,2N ⁻ ,N _{im}

^a Estimated errors of EPR parameters: $\Delta g_{xx} = \Delta g_{yy} = \pm 0.002$, $\Delta g_{zz} = \pm 0.001$, $\Delta A_{xx} = \Delta A_{yy} = \pm 0.5$ G, $\Delta A_{zz} = \pm 0.2$ G

^{b,c,d} These species were treated with identical EPR spectra, see text

^e The EPR spectra of these species are broad singlet, therefore the number of bound nitrogens cannot be determined (in fact, several isomers may exist in the solution).

^f These species possess two separated copper(II) centers (comp.1 and comp.2) with different coordination environments and the three differently protonated complexes were treated with an identical EPR spectrum, see text

Table 3. IC₅₀ (μM) values of the Cu(II)-L system, the native Cu,Zn-SOD enzyme and some of the most active histidine-based SOD-mimicking compounds reported so far.

Complex	IC ₅₀ (μM)	ref.
Cu,Zn-SOD (pH = 6.8)	0.0045	31
Cu(II)-Ac-HSaHSaHSaH-NH ₂ ; 1/1 (pH = 7.4) ^a	0.044	41
Cu(II)-HADHDHKK-NH ₂ ; 1/1 (pH 7.0)	0.11	This work
Cu(II)-Ac-(PHGGGWGQ) ₄ -NH ₂ ; 1/1 (pH = 6.6)	0.12	42
Cu(II)-Ac-HHGH-OH ; 1/1 (pH 6.8)	0.13	31
Cu(II)- HGDHMHNHDTK-NH ₂ ; 1/1 (pH 7.0)	0.19	12
Cu(II)-Ac-HVH-NH ₂ ; 1/1 (pH 7.4)	0.20	43
Cu(II)-carnosine ; 1/1000 (pH 7.4)	0.80	44
Cu(HPO ₄) (pH = 7.4)	1.06	43

^a Sarcosine (Sa) containing peptide

Legends

Fig. 1. Speciation diagrams of the zinc(II)–**L** system ($[\text{Zn}^{2+}] = [\text{L}] = 0.0015 \text{ M}$, $T = 298 \text{ K}$, $I = 0.1 \text{ M NaCl}$).

Fig. 2. ^1H NMR spectra of **L** in D_2O ($T = 298 \text{ K}$) as a function of increasing zinc(II) concentration at $\text{pH}^* = 7.0$.

Fig. 3. pH-dependent UV-Vis spectra of the copper(II)–**L** system. $[\text{Cu}^{2+}]_{\text{tot}}/[\text{L}]_{\text{tot}} = 1/1$ (A) and $2/1$ (B). The inserts show the pH-A profiles at 310 (●) and 550 nm (■). ($[\text{L}] = 1.5 \times 10^{-3} \text{ M}$ (A and B), $I = 0.1 \text{ M NaCl}$, $T = 298 \text{ K}$.)

Fig. 4. pH-dependent CD spectra of the copper(II)–**L** system. $[\text{Cu}^{2+}]_{\text{tot}}/[\text{L}]_{\text{tot}} = 1/1$ (A) and $2/1$ (B). The inserts show the pH- ΔA profiles at 310 (■), 500 (◆) and 600 (▲) nm. ($[\text{L}] = 1.5 \times 10^{-3} \text{ M}$ (A and B), $I = 0.1 \text{ M NaCl}$, $T = 298 \text{ K}$)

Fig. 5. Speciation diagrams of the copper(II)–**L** system.

$[\text{Cu}^{2+}]_{\text{tot}}/[\text{L}]_{\text{tot}} = 1/1$ (A), $2/1$ (B) and $1/2$ (C). ($[\text{L}] = 0.001 \text{ M}$, $T = 298 \text{ K}$, $I = 0.1 \text{ M NaCl}$, the species are denoted by their pqr numbers).

Fig. 6. pH dependence of anisotropic EPR spectra ($T = 77 \text{ K}$, $I = 0.1 \text{ M NaCl}$, $[\text{L}] = 1.2 \text{ mM}$, $[\text{Cu}^{2+}]/[\text{L}] = 1/1.2$ (A), $2/1$ (B)) detected in the copper(II)–**L** systems (black) together with the simulated curves (grey).

Fig. 7. Inhibition of the Nitroblue Tetrazolium (NBT) reduction by superoxide as a function of the concentration of copper(II) complexes ($[\text{Cu}^{2+}] = [\text{L}]$, 0.05 M phosphate buffer, pH = 7.0).

Fig. 8. The most stable calculated structures for the ZnH_2L (A) and accepted for CuH_2L (B) species (the axially coordinated water molecules in B are neglected for clarity)